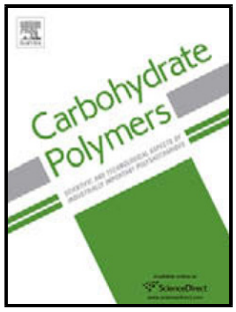

Title: Mineralized alginate hydrogels using marine carbonates for bone tissue engineering applications

Authors: P. Diaz-Rodriguez, P. Garcia-Triñanes, M.M. Echezarreta López, A. Santoveña, M. Landin

PII: S0144-8617(18)30495-8
DOI: https://doi.org/10.1016/j.carbpol.2018.04.101
Reference: CARP 13555

To appear in:

Received date: 5-3-2018
Revised date: 24-4-2018
Accepted date: 26-4-2018

Please cite this article as: Diaz-Rodriguez, P., Garcia-Triñanes, P., López, MM Echezarreta., Santoveña, A., & Landin, M., Mineralized alginate hydrogels using marine carbonates for bone tissue engineering applications.*Carbohydrate Polymers* https://doi.org/10.1016/j.carbpol.2018.04.101

Mineralized alginate hydrogels using marine carbonates for bone tissue engineering applications

Diaz-Rodriguez P[1,2*], Garcia-Triñanes P[3], Echezarreta-López MM[4], Santoveña A[4], Landin M[1]

[1]Dpto. Farmacología, Farmacia y Tecnología Farmacéutica, R+D Pharma Group (GI-1645), Facultad de Farmacia, University of Santiago de Compostela, Santiago de Compostela, Spain

[2]Instituto de Bioingeniería en Red para el Envejecimiento Saludable-IBEROS Network, Spain

[3]Faculty of Engineering and Science, University of Greenwich, UK

[4]Dpto. Ingeniería Química y Tecnología Farmacéutica. Sección de Farmacia. University of La Laguna, La Laguna, Spain

[*]**Corresponding author**:

Patricia Díaz-Rodríguez

Departamento de Farmacología, Farmacia y Tecnología Farmacéutica, R+DPharma Group (GI-1645), Facultad de Farmacia, Universidade de Santiago de Compostela, 15782 Santiago de Compostela, Spain.

Email: patricia.diaz.rodriguez@usc.es Tel: +34 881815252. Fax: +34 881815106

Highlights:

- $CaCO_3$ mineralized alginate hydrogels promoted osteogenic differentiation of MSCs
- Alginate composition modulates hydrogel mechanical properties and cell responses
- $CaCO_3$ particle characteristics depend on the source material selected for production

Abstract

The search for an ideal bone tissue replacement has led to the development of new composite materials designed to simulate the complex inorganic/organic structure of bone. The present work is focused on the development of mineralized calcium alginate hydrogels by the addition of marine derived calcium carbonate biomineral particles. Following a novel approach, we were able to obtain calcium carbonate particles of high purity and complex micro and nanostructure dependent on the source material. Three different types of alginates were selected to develop inorganic/organic scaffolds in order to correlate alginate composition with scaffold properties and cell behavior. The incorporation of calcium carbonates into alginate networks was able to promote extracellular matrix mineralization and osteoblastic differentiation of mesenchymal stem cells when added at 7 mg/ml. We demonstrated that the selection of the alginate type and calcium carbonate origin is crucial to obtain adequate systems for bone tissue engineering as they modulate the mechanical properties and cell differentiation.

Keywords: biominerals, mineralization, bone, hydrogel, marine carbonate particles, tissue engineering

1. Introduction

Biominerals are biologically produced minerals that provide strength and defense to living organisms. They form endo- and exoskeletons and are the main structural components of the dentition system. Apatites are the most common biomineral in vertebrates whereas calcium carbonates ($CaCO_3$) are the major forms of biominerals in invertebrates (Gopinathan et al., 2014). The main structural tissue of the skeletal system in vertebrates is bone. The complex composition of bone, formed by an inorganic phase, hydroxyapatite (HAp), embedded in an organic phase, mainly collagen type I, is responsible for its bending, compression and elongation strength (Blitterswijk C, 2008).

The use of hydrogels as scaffolds for bone tissue engineering shows several advantages; mechanical stability, gradual degradation able to be coupled with tissue regeneration, possibility to be used for the repair of irregular shape defects using minimally invasive surgery and ability to carry small molecules and controlled release them through the intrinsic transport properties of the gel (Guarino, Galizia, Alvarez-Perez, Mensitieri, & Ambrosio, 2015; Kim, Kang, Mercado-Pagan, Maloney, & Yang, 2014; Pasqui, Torricelli, De Cagna, Fini, & Barbucci, 2014). Taking advantage of these properties, different strategies have been focused on the development of hydrogels useful for drug release and tissue replacement in a wide variety of biological systems as nucleus pulposus, central nervous system, cartilage and bone (El-Sherbiny & Yacoub, 2013; Gharat et al., 2018; Giordano et al., 2009; Reitmaier et al., 2012). One of the requirements for biomaterials bone integration is bioactivity, defined as the ability of a biomaterial to promote the formation of a hydroxyapatite layer (Magalhaes et al., 2013). Numerous authors have attempted to go a step further and mimic the natural bone mineralization by the incorporation of salt crystals or the nucleation and growth of inorganic minerals inside a polymeric matrix (Douglas Timothy, Pamula, & Leeuwenburgh Sander, 2013). This biomineralization process aims to obtain organic/inorganic hybrid hydrogels that resemble bone extracellular matrix (ECM) composition (Huh, Zhao, & Kim, 2015). Different polymers can be used for this approach such as; chitosan (Diaz-Dosque et al., 2008; Munro, Green, Dangerfield, & McGrath, 2011), alginate (Diaz-Dosque et al., 2008; Wang, Leng, Che, & Shao, 2010; Xie et al., 2010), κ-carragenan (Diaz-Dosque et al., 2008) or synthetic polymers (Cha, Kim, Kim, & Kong, 2011; Guarino et al., 2015; Pasqui et al., 2014; Phadke, Shih, & Varghese, 2012). These composites are characterized by a high biocompatibility and their ability to promote osteogenic differentiation of mesenchymal stem cells (Pasqui et al., 2014; Phadke et al., 2012).

Polysaccharides are polymers that can easily interact with water, cations and tissue components such as proteins. They form viscous solutions in water and, under some specific conditions, viscoelastic gels. The mechanical properties of those gels can be modulated by the ionic concentration of the solvent used and the molecular weight of the polymers selected (J. Park & Lakes, 2007; Rinaudo, 2008; Tiwari, 2010). Alginates are obtained from brown algae or produced by bacteria. They are biocompatible and non-immunogenic polysaccharides (Draget KI, 2010) widely used in tissue engineering (Kuo & Ma, 2001), cell encapsulation (Draget KI, 2010) and drug delivery (Laurienzo, 2010; Rinaudo, 2008; Tiwari, 2010; Zhang et al., 2008) applications. One of the main advantages of alginates is their ability to form stable hydrogels in mild conditions by the simple addition of divalent ions, such as Ca^{+2}, to the polymeric solution. The formation of these hydrogels is dependent on the pH, ion concentration and alginate composition (Hoffman, 2002; Kuo & Ma, 2001; Laurienzo, 2010; Pathak, Yun, Lee, & Paeng, 2010; Russo, Malinconico, & Santagata, 2007). The incorporation of HAp to alginate hydrogels has led to bioactive composite systems with excellent properties for bone tissue engineering (Gkioni, Leeuwenburgh, Douglas, Mikos, & Jansen, 2010).

Different minerals can be used as the inorganic component for the development of biomineralized hydrogels. Calcium phosphates are the most commonly used, due to their similarities with the composition of bone (Gkioni et al., 2010). Moreover, other biominerals as calcium carbonates have also been studied for bone tissue engineering applications. Nature derived calcium carbonate scaffolds, nanoparticles and granules have been explored in the last decade in the tissue engineering field. Calcium carbonate is the main component of mollusk shells. In a similar way to bone, shells are formed by an organic/inorganic composite with a complex macro and microscopic structure responsible for its exceptional mechanical properties (Alakpa et al., 2017; Li, Xin, Muller,

& Estroff, 2009). Calcium carbonates possess better biodegradation rates than HAp while maintaining a suitable mechanical strength which make them appropriate for bone regeneration (Yang et al., 2016). Marine derived scaffolds, mainly formed by calcium carbonate, have been found to be biocompatible and osteoinductive, being able to produce a functional vascularized bone graft when implanted in vivo (Cui et al., 2007; Chen et al., 2004). More recently, the use of marine derived calcium carbonate particles has been analyzed for the control release of cytokines as BMP-2 (Adams, Mostafa, Schwartz, & Boyan, 2014; Shi et al., 2017).

Even though biomineralized hydrogels are able to resemble the composition of bone, natural and synthetic minerals show differences in porosity, thermal and structural properties (Sofronia, Baies, Anghel, Marinescu, & Tanasescu, 2014). Furthermore, these systems are not able to simulate the complex hierarchical architecture of bone at the nano and microscale. In this study, we propose the synthesis of novel biomimetic mineralized calcium alginate hydrogels by the addition of calcium carbonate biomineral microparticles obtained from mollusk shells. This approach should allow for taking advantage of both natural components; Alginate would form the biodegradable polymeric matrix while calcium carbonate would stimulate cell differentiation and mimic tissue nanostructure. The proposed systems are environmental-friendly and inexpensive giving a second use of the shells obtained as waste products of the canning industry and using a marine polysaccharide for the hydrogel network formation.

2. Materials and Methods

2.1. Materials

Sodium alginates following the European Pharmacopeia purity criteria were supplied by Danisco (France). Three varieties were selected for the experiment; GRINDSTED®

Alginate PH 150, GRINDSTED® Alginate PH 127 and GRINDSTED® Alginate PH 155. Anhydrous calcium chloride was purchased from Panreac (Spain).

2.2. Shells powder preparation

Particles of calcium carbonate were produced from residues of farmed mussels and oysters. Shells were pulverized to reduce their particle size and then calcined in an oven at 550°C to remove the organic components of the shells. Initially, shells were crushed using a lab scale Jaw Crusher and, at a later stage, the resulting granules were washed several times, suspended in water and grinded down to particle sizes below 10 μm using a wet attrition mill at a rotation speed of 880 rpm. Mg-PSZ balls of 2 mm in diameter (partially stabilized zirconia with magnesia) were used as the grinding agent. The volume ratio of product/ball was 1/3 and the grind cycle used was 3 hours for 120 g of sample. In between comminution, grinding media were washed with water and ethanol. The sterilization for the in vitro assays was carried out by autoclave (Raypa, Spain).

2.3. Marine $CaCO_3$ particle characterization

In order to corroborate the obtained powders were indeed, formed by calcium carbonate particles, their chemical composition was characterized by powder X-Ray diffraction (pXRD) on a PANalytical X'Pert Pro instrument (Cu kα1). Particle size distribution was analyzed by laser diffraction (Mastersizer X, Malvern Instruments, United Kingdom) while density and surface area of the powders were measured by helium pycnometry (Quantachrome Mod. PY2, USA) and nitrogen adsorption (Micromeritics ASAP 2000, USA) using the Brunauer-Emmett-Teller (BET) method, respectively. Void Fraction was estimated as a function of the real density (ρ_p) and the apparent density (ρ_b) as is shown in Equation 1.

$$\varepsilon = 1 - \frac{\rho_b}{\rho_p}$$

Equation 1: Void fraction quantification

Morphological assessments of the particles were carried out by scanning electron microscopy (SEM). Images were obtained after coating the samples with gold on a SEM Zeiss EVO LS 15 microscope.

2.4. Alginate characterization

2.4.1 ^{1}H Nuclear Magnetic Resonance

In order to correlate the chemical composition of alginates with the properties of the developed hydrogels, the composition of the different alginates was analyzed by Nuclear Magnetic Resonance (NMR). Prior to the analysis, alginate samples were partially hydrolyzed following the methodology described by Andriamanantoanina and co-workers (Andriamanantoanina H, 2010). Briefly, GG (where G is α-L-guluronic acid) and MM (where M is β-D-mannuronic acid) block fractions of alginates were obtained after two separate processes of precipitation and concentration. The hydrolysis yield, expressed as mass percentage (%wt), was calculated by adding the weights of recovered purified GG and MM blocks and diving it by the initial sample weight. The M/G ratio of each alginate was analyzed by ^{1}H NMR as described elsewhere (Grasdalen, 1983; Grasdalen H, 1979). ^{1}H NMR experiments were performed at 85°C on a 6 mg/ml alginate solution in D_2O (Sigma), spectra were recorded using a Bruker DRX 500 spectrometer (Germany) operating at 400.13 MHz. Calibration was performed using the signal of the residual protons of the solvent as a secondary reference.

2.4.2 Alginate Molecular Weight Characterization

Alginates molecular weight was determined using Gel Permeation Chromatography (GPC). Polymeric solutions were prepared at 2.5 g/l in distilled water + 0.1 M $NaNO_3$ + NaN_3 and filtered through 0.45 µm (Chromafill XTra, Macherey-Nagel). Samples were

injected at 0.5 ml/min at 25 °C using an HPLC pump (Waters 515) and an autosampler (Waters 717 plus Autosampler) on a system formed by a pre-column and 3 columns Shodex OH-pak 30 cm (802.5HQ, 804HQ, 806HQ) with a separation range from 100 to 1 800 000 g/mol equipped with a differential refractometer (Waters 2414) and a LS multi-angle mini DAWN TREOS (Wyatt Techn).

2.5. Hydrogel Synthesis

Mineralized calcium alginate hydrogels were prepared as described below. Homogeneous suspensions of marine $CaCO_3$ particles, obtained from mussels (MS) or oysters (OY) shells, were prepared in sterile phosphate buffer pH 7.4 (PBS) at two different concentrations (0.7 or 7 mg/ml) under continuous magnetic stirring. A precise amount of sodium alginate was then dissolved on the particle suspensions to obtain a 1% final alginate concentration. The obtained dispersions were exposed to ultrasound to avoid particle aggregation, transferred into a 7.0 KDa MWCO dialysis tube (Medicell International Ltd, UK) and subsequently immersed in a calcium chloride (1%) solution for 24 hours. Once the cross-linking was complete, hydrogels were washed three times with PBS, removed from the dialysis tube and cut in 1 mm width discs.

2.6 Mechanical properties of cross-linked hydrogels

The compression strength of cross-linked mineralized hydrogels containing different concentrations of calcium carbonate particles was evaluated in quadruplicate using a texturometer (TA.XT Plus, TA Instruments). Compression assessments were performed to 80% strain at 25°C with a deformation rate of 1 mm/s. The Young's modulus was calculated as the slope of the stress-strain curve on the linear region of the curve.

2.7. Cytocompatibility, cell adhesion and extracellular matrix mineralization

The cytocompatibility, cell adhesion, and extracellular matrix mineralization of alginate hydrogels alone or including OY or MS particles (7 mg/ml) were evaluated using a human osteoblast cell line (Saos-2; ATCC® HTB-85™). Cells were cultured with DMEM (Dulbeco´s Modified Eagles Medium) supplemented with 10% of fetal bovine serum and 1% of penicillin/streptomycin.

Hydrogel cytocompatibility was analyzed by placing polymeric discs of variable compositions on the bottom of 24-well plates after which 100,000 cells per well were added. Viable cells were assessed using a commercial cell proliferation kit (MTT, Roche) after 24 hours of culture. To evaluate the possible improvement of cell attachment by the addition of calcium carbonate particles to alginate hydrogels, cellular adhesion to hydrogel surfaces was analyzed after 4 hours of culture. Following a similar protocol as for cytocompatibility assessments, hydrogel discs were placed on 24-well plates and 400,000 cells were added to each well. After 4 hours of incubation hydrogels were removed from the well and transferred to sterile tubes containing 1 ml of hydrogel dissolution medium (55 mM sodium citrate, 0.15 M sodium chloride, 30 mM EDTA) (H. Park et al., 2012) and incubated for 30 minutes. After incubation, tubes were centrifuged at 1400 rpm for 5 minutes, the supernatant was removed and cell pellets were resuspended on 0.4% trypan blue. Finally, the number of viable cells extracted for each hydrogel was quantified using a Neubauer improved chamber (Blau Brand, Germany).

The effect of the incorporation of calcium carbonate particles on hydrogel biomineralization was also evaluated. Human osteoblasts were cultured on hydrogel surfaces at $5x10^4$ cells/cm^2 for five days changing media every other day. The presence of calcium deposits was evaluated performing an Alizarin Red staining. Cells were fixed with EtOH:H_2O (70:30) during 1 hour at 4 °C and then washed twice with ultrapure water. Consequently, Alizarin Red staining was carried out applying a 2% dye solution for 30

minutes followed by washing the samples three times with ultrapure water. The presence of calcified ECM was evaluated using an inverse microscope (Nikon Eclipse TS100).

2.8. hMSCs differentiation

Bone marrow derived mesenchymal stem cells (hMSCs) extracted from human bone marrow aspirates were provided by Instituto de Ortopedia y Banco de Tejidos Musculoesqueléticos of the University of Santiago de Compostela. Cells were cultured with Minimum Essential Media (αMEM) supplemented with 20% of fetal bovine serum and 1% of penicillin/streptomycin. Mineralized hydrogels prepared with Alginate PH 155 as the polymeric component were selected to analyze the effect of hydrogel composition on hMSCs differentiation due to the good experimental results shown in previous studies. Hydrogels containing 0, 0.7 or 7 mg/ml of marine derived calcium carbonates were cultured on 24-well plates with 30,000 hMSCs as shown in Supplementary Figure 1. Cell proliferation after 1 and 5 days of culture was quantified by a commercial cell proliferation kit (MTT, Roche) cell differentiation to preosteblasts was evaluated by the quantification of alkaline phosphatase activity (ALP) using a colorimetric assay (ALP Takara). Hydroxyapatite (HAp) particles at equal concentrations were used as positive controls of differentiation.

2.9 Statistical analysis

Experimental data has been reported as mean ± standard error of the mean. Comparison of samples was performed by one way ANOVA followed by Tukey's post hoc test (IBM SPSS 24 software), samples with a p-value < 0.05 were considered statistically significant different.

3. Results

3.1 Marine $CaCO_3$ particle characterization

The pulverization and calcination of mussel (MS) and oyster (OY) shells led to final powders with different physical properties as a function of the raw material used. However, as expected, the composition of both particle types appears to be identical, mainly formed by calcium carbonate ($CaCO_3$) present as calcite crystals according to the ICDD database patterns and previously reported data (Kontoyannis & Vagenas, 2000; Ni & Ratner, 2008) (Figure 1).

Scanning electron micrographs (Figure 2 A-B) of MS and OY particles pointed out clear differences in morphology. MS particles are characterized by a needle shape with a wide particle size distribution (Figure 2 A, C) whereas OY shells give a product formed by rounded particles with a narrow particle size distribution and a mean size diameter of 1.5 μm (Figure 2 B, D).

Further characterization of the shell powders was performed through helium pycnometry and nitrogen absorption. The changes in particle morphology shown in Figure 2 also led to differences in specific surface area and density. MS particles were characterized by a bulk density of 904 kg/m^3 and a real density of 2650 kg/m^3 which leads to a void faction of 0.65. On the other hand, OY particles showed a lower void fraction (0.57) than MS particles with values of bulk density of 1099 kg/m^3 and real density values of 2540 kg/m^3. Moreover, OY powders have greater specific surface area (14.16 m^2/g) than the ones obtained from MS shells (3.57 m^2/g) most likely due to changes in particle morphology and size which leads to an increase in surface area per mass unit.

3.2 Alginate characterization

Alginate chain characterization was carried out by H^1-NMR. As mentioned in the Materials and Methods section, three different alginates were selected for this study; GRINDSTED® Alginate PH 127 (named 127), GRINDSTED® Alginate PH 150 (named 150) and GRINDSTED® Alginate PH 155 (named 155). Guluronic (GG) and

mannuronic (MM) blocks were obtained by partial acid hydrolysis of the polymers. Divalent cations are believed to promote alginate crosslinking by mainly binding to guluronate blocks as their conformation allows for a higher coordination degree of divalent ions. To understand the crosslinking of the different alginate solutions with the addition of Ca^{+2} we analyzed the M/G ratio of alginates by H^1-NMR (Table 1, Supplementary Figure 2). All the varieties of alginates analyzed showed similar M/G ratios.

Table 2 shows the purity of both GG and MM block for the three types of alginate, determined by the percentage of GG or MM content of each block respectively. The purity obtained for all the blocks was higher that 75%. Values of number-average degree of polymerization (DPn) for each block and polymer were obtained from the integral of anomeric protons compared with H-1 of G units or with H-5 of M units as previously reported by Andriamanantoanina and Rinaudo 2010 (Andriamanantoanina H, 2010). Alginate 127 is characterized by the highest DPn values for GG and MM blocks followed by Alginate 150 and lastly Alginate 155 (Table 2).

3.3 Mechanical properties of cross-linked hydrogels

Mineralization modifies tissue mechanical properties determining compressive modulus (Koburger et al., 2014). The compression strength of the cross-linked alginate hydrogels alone or containing both calcium carbonate particles at a concentration of 7 mg/ml were assessed. The experimental data (Figure 3) showed an effect of not only the addition of calcium carbonate particles but also the alginate type on the mechanical behavior of the hydrogels. Alginate 127 and 155 were characterized by an average Young's modulus of 6 kPa that could be increased by the addition of ceramic particles. The incorporation of MS or OY to both alginate hydrogels was able to increase the compression modulus in a

similar way, obtaining a 1.5-fold increase in Young's modulus for both alginates when MS calcium carbonate particles were added to alginate solutions previous to cross-linking. On the contrary, the presence of calcium carbonate particles (MS and OY) on alginate 150 hydrogels promoted a decrease on the compression strength of the hydrogels. Hydrogels of alginate 150 alone showed an average Young's modulus of 12 kPa whereas the gels formed by alginate 150 + MS were characterized by a Young's modulus of 8.9 kPa while for the ones including OY particles + alginate 150 it was 5kPa.

3.4 Cytocompatibility, cell adhesion and ECM mineralization

Alginate is a well-known polymer in the regenerative medicine field because of its high biocompatibility and low toxicity. However, it behaves as a cell resistant material, not allowing cells to attach to the polymeric surface (Morra & Cassinelli, 2002; Sakai, Hirose, Moriyama, & Kawakami, 2010). Figure 4A shows osteoblasts cell viability when cultured with the different hydrogels. All samples showed similar cell viability values after 24 hours of culture. However, the hydrogels formed by Alginate 150 were the ones with lower cell viability values finding statistically significant differences when Alginate 150 hydrogels were compared to Alginate 127 MS (p-value = 0.049) and when Alginate 150 OY formulations were compared to Alginate 127 (p-value = 0.048) and Alginate 127 MS (p-value = 0.006).

In order to evaluate the potential increase on osteoblasts cell adhesion with the incorporation of calcium carbonate particles, cells were seeded onto the surface of crosslinked hydrogels and the number of attached cells was analyzed after 4 hours of culture. Figure 4B shows the normalized cell attachment of the developed hydrogels to easily visualize the effect of $CaCO_3$ particles incorporation on cell adhesion. The normalization was performed dividing the number of attached cells on each mineralized hydrogel by the correspondent number of attached cells on the hydrogels without ceramic

particles. The incorporation of MS or OY particles into Alginate 150 did not promote any change in cell attachment. However, the addition of MS particles to Alginate 127 and Alginate 155 promoted an increase in cell attachment even though it was not statistically significant. Interestingly, the addition of OY particles to Alginate 127 and Alginate 155 not only did not improve cell attachment but also produced a significant decrease in cell attachment when compared to mineralized hydrogels including OY particles and their correspondent alginates. Our experimental data demonstrated the selection of the alginate type and calcium carbonate origin is crucial to obtain adequate systems for tissue engineering.

The addition of inorganic particles to alginate hydrogels could also led to an improvement in ECM mineralization, crucial for bone repair and tissue engineering. Osteoblasts were cultured with the developed hydrogels for five days. The presence of calcium deposits was evaluated through Alizarin Red staining using an inverted miscroscope. As shown in Figure 5, the incorporation of MS and OY particles to a final concentration of 7 mg/ml was able to increase ECM mineralization for all the hydrogels independently of the alginate type selected.

3.5. hMSCs differentiation

The potential osteoblastic differentiation of mesenchymal stem cells was evaluated by the quantification of alkaline phosphatase activity, an early differentiation marker. For these experiments Alginate 155 (MW 4.19 ± 0.015 10^5 g/mol according to GPC data) was selected as the polymeric component of the hydrogel containing variable concentrations of ceramic particles. Hydroxyapatite particles (HAp) were also assayed and used as positive controls for differentiation. The incorporation of ceramic particles at 0.7 mg/ml to the polymeric systems was not able to significantly increase the activity of ALP (Figure 6). However, when the concentration of the particles selected was ten-fold higher, a

significant increase in ALP activity could be observed for hydrogels containing OY and HAp particles when compared to non-mineralized hydrogels, p-values of 0.013 and 0.031 respectively. In agreement with Alizarin Red staining images, these data suggest that ceramic particles should be incorporated at higher concentrations than 0.7 mg/ml into alginate hydrogels to observe an effect in ECM calcification and osteoblastic differentiation of MSCs.

4. Discussion

Mollusk shells are mainly composed by calcium carbonate (95%) with a 5% of organic material. This natural composite is characterized by extraordinary mechanical properties and a unique porous microstructure. Calcium carbonate could be present as calcite or aragonite polymorphs in mollusk shells depending on numerous variables as temperature, food availability, wave exposure or predation pressure (McCoy, Kamenos, Chung, Wootton, & Pfister, 2018; Zhou et al., 2017). XRD data demonstrated the produced MS and OY powders were mainly formed by calcium carbonate present as the most stable polymorph, calcite. We were able to obtain $CaCO_3$ particles of high purity following an environmentally friendly and inexpensive protocol giving a second used for waste products.

Differences in particle size and morphology of the powders obtained from different natural sources were observed. The pulverization of oyster shells led to particles of small size and round morphology whereas mussel shells produced needle shaped particles. The milling protocol followed in this work was able to improve particle size distribution when compared to previously published data of mollusk shells $CaCO_3$ particles obtaining a narrow particle size distribution especially for OY particles (Hamester, Balzera, & Becker, 2012).

Even though alginates are widely used in tissue engineering less is known about the correlation of alginate properties and cell responses. To address this issue, we decided to perform the experiments using three different alginates with variable viscosities according the manufacturer characterization. Alginates were analyzed by NMR and, as expected, different degrees of polymerization were obtained for the blocks of each polymer. When analyzing the mechanical properties of the hydrogels obtained with the three alginate varieties at the same polymer and Ca^{+2} concentration we could observed that Alginate 150 showed the highest Young's modulus. This behavior could be correlated to the low degree of polymerization observed for both Alginate 150 GG and MM blocks together with the low M/G ratio of the polymer. On this context, the addition of calcium carbonate particles to Alginate 150 could partially disrupt the polymeric network and cause a decrease in compression strength as observed in Figure 2. This effect was not observed for neither Alginate 127 nor Alginate 155. They could form a less compact hydrogel network in which the incorporation of ceramic particles would improve the mechanical properties of the hydrogel as reported previously for similar systems (You, Li, Zhou, Liu, & Zhang, 2016).

All the hydrogels were characterized by high values of cell viability as expected for biocompatible materials. The presence of calcium carbonate on the hydrogel network did not increase cell death. These results indicate the absence of toxic substances in the processed materials. However, hydrogels formed by Alginate 150 showed lower cell viability when compared to Alginate 127. It has been reported that calcium alginate hydrogels with high G content are more immunogenic in vivo than hydrogels with intermediate G content (Tam et al., 2011). This fact could explain the observed effect of Alginate 150 (M/G ratio 0.51) on cell viability when compared to Alginate 127 (M/G ratio 0.61).

Marine derived scaffolds, mainly formed by calcium carbonate, have been explored recently for tissue engineering applications. Numerous studies have shown their excellent bioactivity, osteointegration and osteoinduction (Alakpa et al., 2017; Chroscicka et al., 2016; Decambron et al., 2017; Weiss et al., 2017). In this study we reported the ability of calcium carbonate particles derived from invertebrate shells to promote ECM mineralization and osteoblastic differentiation of MSC when incorporated at 7 mg/ml into alginate hydrogels. Although no significant effect on cell adhesion was observed with the addition of $CaCO_3$ particles to alginate, the presence of OY particles into the polymer network was able to significantly increase ALP activity of MSC to a similar level to that of alginate-HAp hydrogels. In agreement to previously reported data, $CaCO_3$ particles showed an osteoinductivity comparable to HAp with improved biodegradation properties (Suzawa et al., 2010). This osteoinductive potential of marine-derived scaffolds has been hypothesized to be related to the surface patterns presented to mesenchymal stem cells (Alakpa et al., 2017). The different morphological and surface properties of MS and OY particles observed in the initial $CaCO_3$ characterization step could explain the differences in osteogenic potential among them.

Conclusions

We were able to successfully develop high biocompatible mineralized alginate hydrogels. To the best of our knowledge these are the first mineralized hydrogels that include calcium carbonate biomineral particles for tissue engineering applications. The mechanical properties and cell responses of these systems could be tailored by changing the type of alginate, the natural source selected to obtain the biologically produced mineral and the concentration of microparticles in the network. The selection of Alginate 155 hydrogels containing 7 mg/ml of OY particles was able to promote the osteogenic differentiation of hMSCs. Thus, the incorporation of calcium carbonate particles into

alginate networks was able to modulate hMSCs differentiation. Furthermore, the presence of $CaCO_3$ in the alginate matrix could improve long term stability of alginate hydrogels as the partial dissolution of calcium carbonate crystals would led to the release of Ca^{+2} ions that promote alginate gelation.

Acknowledgments

Authors thank Dr Mónica Gómez Boado and Prof. Francisco Guitián Rivera (Instituto de Cerámica de Galicia) for kindly assist in the preparation of the solid calcium carbonate samples. Authors also thank Interreg V-A POCTEP Program (0245_IBEROS_1_E) of EU (FEDER) for financial support.

Limitations

All the hydrogel formulations were freshly prepared for the experiments. However, we did not control for syneresis.

References

Adams, B. R., Mostafa, A., Schwartz, Z., & Boyan, B. D. (2014). Osteoblast response to nanocrystalline calcium hydroxyapatite depends on carbonate content. J Biomed Mater Res A, 102(9), 3237-3242.

Alakpa, E. V., Burgess, K. E. V., Chung, P., Riehle, M. O., Gadegaard, N., Dalby, M. J., & Cusack, M. (2017). Nacre Topography Produces Higher Crystallinity in Bone than Chemically Induced Osteogenesis. ACS Nano, 11(7), 6717-6727.

Andriamanantoanina, H., & Rinaudo, M. (2010). Relationship between the molecular structure of alginates and their gelation in acidic conditions. Polym Int., 59(11), 11.

Andriamanantoanina H, R. M. (2010). Relationship between the molecular structure of alginates and their gelation in acidic conditions. Polym Int., 59(11), 11.

Blitterswijk C, T. P., Lindahl A, Hubbell JA, Williams D, Cancedda R. (2008). Tissue engineering. 1st Ed: Elsevier.

Cui, L., Liu, B., Liu, G., Zhang, W., Cen, L., Sun, J., . . . Cao, Y. (2007). Repair of cranial bone defects with adipose derived stem cells and coral scaffold in a canine model. Biomaterials, 28(36), 5477-5486.

Cha, C., Kim, E. S., Kim, I. W., & Kong, H. (2011). Integrative design of a poly(ethylene glycol)-poly(propylene glycol)-alginate hydrogel to control three dimensional biomineralization. Biomaterials, 32(11), 2695-2703.

Chen, F., Chen, S., Tao, K., Feng, X., Liu, Y., Lei, D., & Mao, T. (2004). Marrow-derived osteoblasts seeded into porous natural coral to prefabricate a vascularised bone graft in the shape of a human mandibular ramus: experimental study in rabbits. Br J Oral Maxillofac Surg, 42(6), 532-537.

Chroscicka, A., Jaegermann, Z., Wychowanski, P., Ratajska, A., Sadlo, J., Hoser, G., . . . Lewandowska-Szumiel, M. (2016). Synthetic Calcite as a Scaffold for Osteoinductive Bone Substitutes. Ann Biomed Eng, 44(7), 2145-2157.

Decambron, A., Fournet, A., Bensidhoum, M., Manassero, M., Sailhan, F., Petite, H., . . . Viateau, V. (2017). Low-dose BMP-2 and MSC dual delivery onto coral scaffold for critical-size bone defect regeneration in sheep. J Orthop Res, 35(12), 2637-2645.

Diaz-Dosque, M., Aranda, P., Darder, M., Retuert, J., Yazdani-Pedram, M., Arias, L. J., & Ruiz-Hitzky, E. (2008). Use of biopolymers as oriented supports for the stabilization of different polymorphs of biomineralized calcium carbonate with complex shape. J Cryst Growth, 310(24), 10.

Douglas Timothy, E. L., Pamula, E., & Leeuwenburgh Sander, C. G. (2013). Biomimetic Mineralization of Hydrogel Biomaterials for Bone Tissue Engineering. In W. X. Ramalingam Murugan, ChenGuoping, Ma Peter, Cui Fu-Zhai (Ed.), Biomimetics: Advancing Nanobiomaterials and Tissue Engineering (pp. 51-67): Wiley

Draget KI, T. C. (2010). Chemical, physical and biological properties of alginates and their biomedical implications. Food Hydrocolloids, 25(2), 6.

El-Sherbiny, I. M., & Yacoub, M. H. (2013). Hydrogel scaffolds for tissue engineering: Progress and challenges. Glob Cardiol Sci Pract, 2013(3), 316-342.

Gharat, T. P., Diaz-Rodriguez, P., Erndt-Marino, J. D., Jimenez Vergara, A. C., Munoz Pinto, D. J., Bearden, R. N., . . . Hahn, M. S. (2018). A canine in vitro model for evaluation of marrow-derived mesenchymal stromal cell-based bone scaffolds. J Biomed Mater Res A.

Giordano, C., Albani, D., Gloria, A., Tunesi, M., Batelli, S., Russo, T., . . . Cigada, A. (2009). Multidisciplinary perspectives for Alzheimer's and Parkinson's diseases:

hydrogels for protein delivery and cell-based drug delivery as therapeutic strategies. Int J Artif Organs, 32(12), 836-850.

Gkioni, K., Leeuwenburgh, S. C., Douglas, T. E., Mikos, A. G., & Jansen, J. A. (2010). Mineralization of hydrogels for bone regeneration. Tissue Eng Part B Rev, 16(6), 577-585.

Gopinathan, G., Jin, T., Liu, M., Li, S., Atsawasuwan, P., Galang, M. T., . . . Diekwisch, T. G. (2014). The expanded amelogenin polyproline region preferentially binds to apatite versus carbonate and promotes apatite crystal elongation. Front Physiol, 5, 430.

Grasdalen, H. (1983). High-field, proton NMR spectroscopy of alginate: sequential structure and linkage conformations. Carbohydr Res, 118(6), 255.

Grasdalen H, L. B., Smidsroed O. (1979). A proton magnetic resonance study of the composition and sequence of uronate residues in alginates. Carbohydr Res, 68(1), 9.

Guarino, V., Galizia, M., Alvarez-Perez, M., Mensitieri, G., & Ambrosio, L. (2015). Improving surface and transport properties of macroporous hydrogels for bone regeneration. J Biomed Mater Res A, 103(3), 1095-1105.

Hamester, M. R. R., Balzera, P. S., & Becker, D. (2012). Characterization of Calcium Carbonate Obtained from Oyster and Mussel Shells and Incorporation in Polypropylene. Materials Research, 15(2), 5.

Hoffman, A. S. (2002). Hydrogels for biomedical applications. Adv Drug Deliv Rev, 54(1), 3-12.

Huh, H. W., Zhao, L., & Kim, S. Y. (2015). Biomineralized biomimetic organic/inorganic hybrid hydrogels based on hyaluronic acid and poloxamer. Carbohydr Polym, 126, 130-140.

Kim, S., Kang, Y., Mercado-Pagan, A. E., Maloney, W. J., & Yang, Y. (2014). In vitro evaluation of photo-crosslinkable chitosan-lactide hydrogels for bone tissue engineering. J Biomed Mater Res B Appl Biomater, 102(7), 1393-1406.

Kontoyannis, C. G., & Vagenas, N. V. (2000). Calcium carbonate phase analysis using XRD and FT-Raman spectroscopy. Analyst, 125, 5.

Kuo, C. K., & Ma, P. X. (2001). Ionically crosslinked alginate hydrogels as scaffolds for tissue engineering: part 1. Structure, gelation rate and mechanical properties. Biomaterials, 22(6), 511-521.

Laurienzo, P. (2010). Marine polysaccharides in pharmaceutical applications: an overview. Mar Drugs, 8(9), 2435-2465.

Li, H., Xin, H. L., Muller, D. A., & Estroff, L. A. (2009). Visualizing the 3D internal structure of calcite single crystals grown in agarose hydrogels. Science, 326(5957), 1244-1247.

Magalhaes, J., Sousa, R. A., Mano, J. F., Reis, R. L., Blanco, F. J., & San Roman, J. (2013). Synthesis and characterization of sensitive hydrogels based on semi-interpenetrated networks of poly[2-ethyl-(2-pyrrolidone) methacrylate] and hyaluronic acid. J Biomed Mater Res A, 101(1), 157-166.

McCoy, S. J., Kamenos, N. A., Chung, P., Wootton, T. J., & Pfister, C. A. (2018). A mineralogical record of ocean change: Decadal and centennial patterns in the California mussel. Glob Chang Biol.

Morra, M., & Cassinelli, C. (2002). Cell Adhesion Micropatterning by Plasma Treatment of Alginate Coated Surfaces. Plasmas Polym, 7(2), 13.

Munro, N. H., Green, D. W., Dangerfield, A., & McGrath, K. M. (2011). Biomimetic mineralisation of polymeric scaffolds using a combined soaking and Kitano approach. Dalton Trans, 40(36), 9259-9268.

Ni, M., & Ratner, B. D. (2008). Differentiation of Calcium Carbonate Polymorphs by Surface Analysis Techniques - An XPS and TOF-SIMS study. Surf Interface Anal, 40(10), 1356-1361.

Park, H., Kim, P. H., Hwang, T., Kwon, O. J., Park, T. J., Choi, S. W., . . . Kim, J. H. (2012). Fabrication of cross-linked alginate beads using electrospraying for adenovirus delivery. Int J Pharm, 427(2), 417-425.

Park, J., & Lakes, R. S. (2007). Biomaterials an introduction 3er Ed. New York: Springer.

Pasqui, D., Torricelli, P., De Cagna, M., Fini, M., & Barbucci, R. (2014). Carboxymethyl cellulose-hydroxyapatite hybrid hydrogel as a composite material for bone tissue engineering applications. J Biomed Mater Res A, 102(5), 1568-1579.

Pathak, T. S., Yun, J., Lee, J., & Paeng, K. (2010). Effect of calcium ion (cross-linker) concentration on porosity, surface morphology and thermal behavior of calcium alginates prepared from algae (Undaria pinnatifida). Carbohydr Polym, 81(3), 7.

Phadke, A., Shih, Y. R., & Varghese, S. (2012). Mineralized synthetic matrices as an instructive microenvironment for osteogenic differentiation of human mesenchymal stem cells. Macromol Biosci, 12(8), 1022-1032.

Reitmaier, S., Shirazi-Adl, A., Bashkuev, M., Wilke, H. J., Gloria, A., & Schmidt, H. (2012). In vitro and in silico investigations of disc nucleus replacement. J R Soc Interface, 9(73), 1869-1879.

Rinaudo, M. (2008). Main properties and current applications of some polysaccharides as biomaterials. Polym Int, 57(3), 4.

Russo, R., Malinconico, M., & Santagata, G. (2007). Effect of cross-linking with calcium ions on the physical properties of alginate films. Biomacromolecules, 8(10), 3193-3197.

Sakai, S., Hirose, K., Moriyama, K., & Kawakami, K. (2010). Control of cellular adhesiveness in an alginate-based hydrogel by varying peroxidase and H(2)O(2) concentrations during gelation. Acta Biomater, 6(4), 1446-1452.

Shi, P., Abbah, S. A., Chuah, Y. J., Li, J., Zhang, Y., He, P., . . . Goh, J. C. H. (2017). Yolk shell nanocomposite particles as bioactive bone fillers and growth factor carriers. Nanoscale, 9(38), 14520-14532.

Sofronia, A. M., Baies, R., Anghel, E. M., Marinescu, C. A., & Tanasescu, S. (2014). Thermal and structural characterization of synthetic and natural nanocrystalline hydroxyapatite. Mater Sci Eng C Mater Biol Appl, 43, 153-163.

Suzawa, Y., Funaki, T., Watanabe, J., Iwai, S., Yura, Y., Nakano, T., . . . Akashi, M. (2010). Regenerative behavior of biomineral/agarose composite gels as bone grafting materials in rat cranial defects. J Biomed Mater Res A, 93(3), 965-975.

Tam, S. K., Dusseault, J., Bilodeau, S., Langlois, G., Halle, J. P., & Yahia, L. (2011). Factors influencing alginate gel biocompatibility. J Biomed Mater Res A, 98(1), 40-52.

Tiwari, A. (2010). Polysaccharides: Development, Properties and Applications.: Nova Science Publishers.

Wang, T., Leng, B., Che, R., & Shao, Z. (2010). Biomimetic synthesis of multilayered aragonite aggregates using alginate as crystal growth modifier. Langmuir, 26(16), 13385-13392.

Weiss, O. E., Hendler, R. M., Canji, E. A., Morad, T., Foox, M., Francis, Y., . . . Baranes, D. (2017). Modulation of scar tissue formation in injured nervous tissue cultivated on surface-engineered coralline scaffolds. J Biomed Mater Res B Appl Biomater.

Xie, M., Olderoy, M. O., Andreassen, J. P., Selbach, S. M., Strand, B. L., & Sikorski, P. (2010). Alginate-controlled formation of nanoscale calcium carbonate and

hydroxyapatite mineral phase within hydrogel networks. Acta Biomater, 6(9), 3665-3675.

Yang, N., Zhong, Q., Zhou, Y., Kundu, S. C., Yao, J., & Cai, Y. (2016). Controlled degradation pattern of hydroxyapatite/calcium carbonate composite microspheres. Microsc Res Tech, 79(6), 518-524.

You, H. J., Li, J., Zhou, C., Liu, B., & Zhang, Y. G. (2016). A honeycomb composite of mollusca shell matrix and calcium alginate. Colloids Surf B Biointerfaces, 139, 100-106.

Zhang, L. F., Yang, D. J., Chen, H. C., Sun, R., Xu, L., Xiong, Z. C., . . . Xiong, C. D. (2008). An ionically crosslinked hydrogel containing vancomycin coating on a porous scaffold for drug delivery and cell culture. Int J Pharm, 353(1-2), 74-87.

Zhou, X., Liu, W., Zhang, J., Wu, C., Ou, X., Tian, C., . . . Dang, Z. (2017). Biogenic Calcium Carbonate with Hierarchical Organic-Inorganic Composite Structure Enhancing the Removal of Pb(II) from Wastewater. ACS Appl Mater Interfaces, 9(41), 35785-35793.

Figure legends:

Figure 1: Particle chemical composition of MS (A) and OY (B) powders obtained by powder X-Ray diffraction.

Figure 2 A-B: Scanning electron micrographs of pulverized calcium phosphate samples from (A) MS and (B) OY shells. **Figure 2 C-D:** Particle size distribution of (C) MS and (D) OY powders after the pulverization process.

Figure 3: Compressive strength (Young's modulus) of crosslinked hydrogels containing calcium carbonate particles. '$' denotes significant difference relative to Alginate 127 MS and '#' denotes significant difference relative to Alginate 150.

Figure 4: Cell viability (A) and Relative Cell Attachment (B) of human osteoblasts (Saos-2) cultured on the surface of mineralized hydrogels. '$' denotes significant difference relative to Alginate 127 and '#' denotes significant difference relative to Alginate 127 MS.

Figure 5: Extracellular matrix mineralization observed by Alizarin Red staining after five days of cell culture with osteoblasts.

Figure 6: Alkaline Phosphatase activity of human mesenchymal cells cultured on Alginate 155 hydrogels containing variable concentrations of calcium carbonate from mussels (MS) or oysters (OY), or HAp particles. '$' denotes significant difference relative to Alginate 155 alone.

.

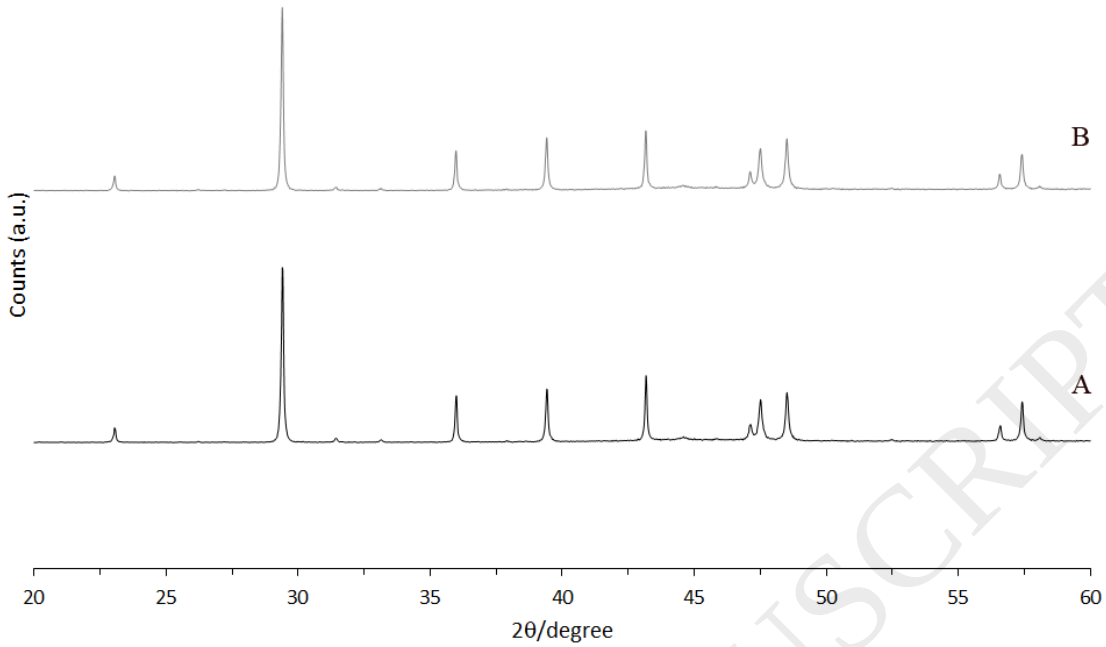

Figure 1: Particle chemical composition of MS (A) and OY (B) powders obtained by powder X-Ray diffraction.

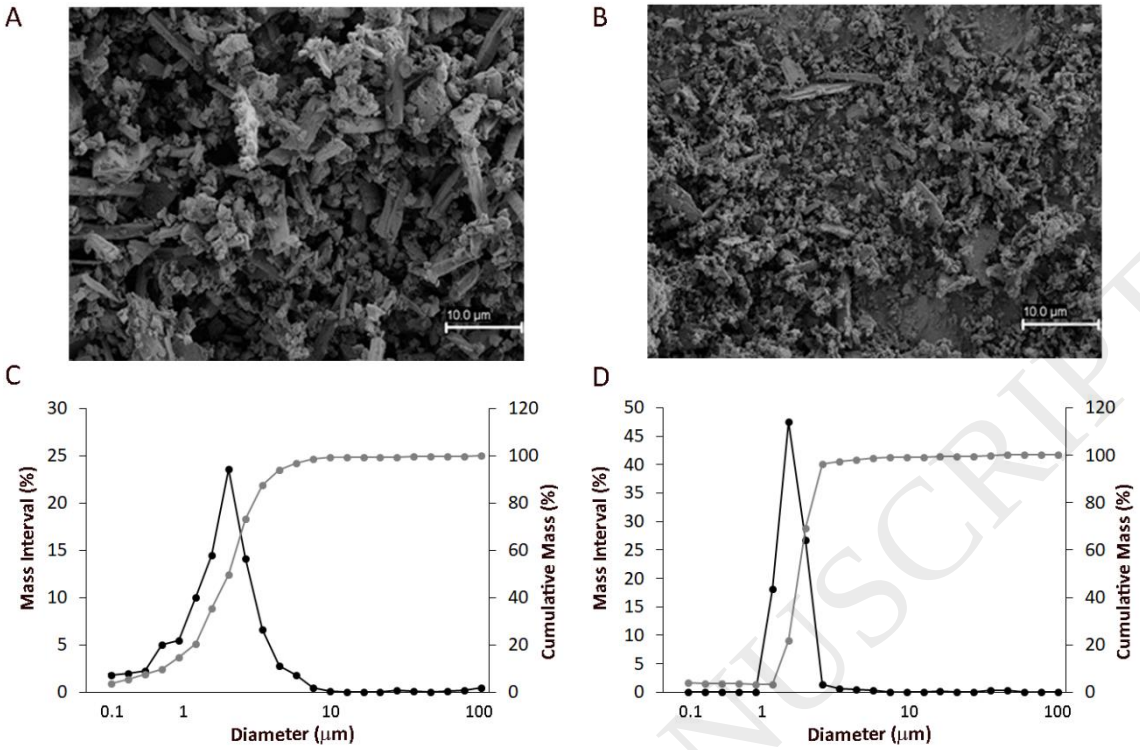

Figure 2 A-B: Scanning electron micrographs of pulverized calcium phosphate samples from (A) MS and (B) OY shells. **Figure 2 C-D:** Particle size distribution of (C) MS and (D) OY powders after the pulverization process.

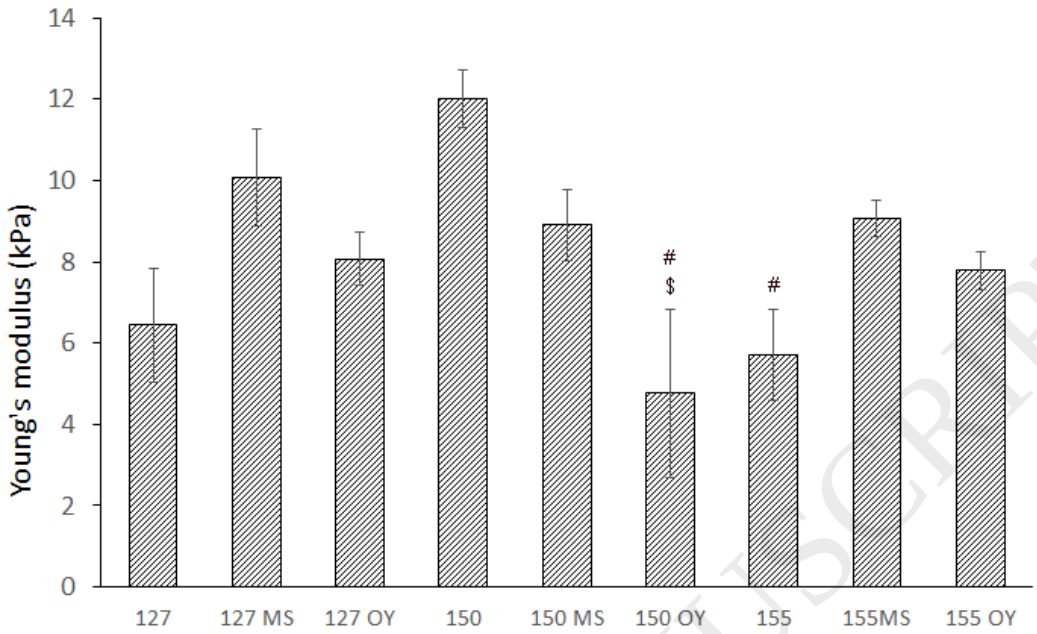

Figure 3: Compressive strength (Young's modulus) of crosslinked hydrogels containing calcium carbonate particles. '$' denotes significant difference relative to Alginate 127 MS and '#' denotes significant difference relative to Alginate 150.

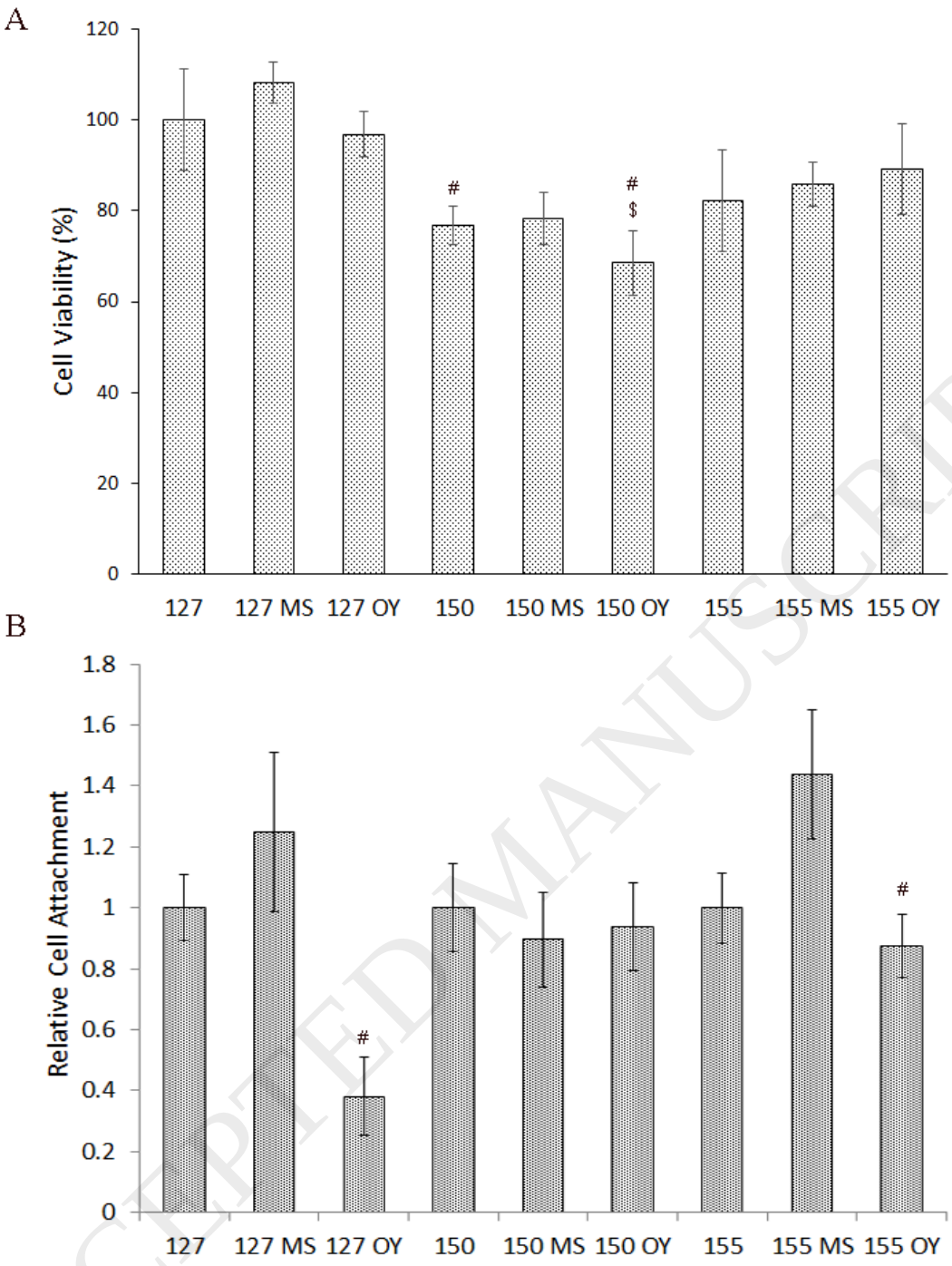

Figure 4: Cell viability (A) and Relative Cell Attachment (B) of human osteoblasts (Saos-2) cultured on the surface of mineralized hydrogels. '$' denotes significant difference relative to Alginate 127 and '#' denotes significant difference relative to Alginate 127 MS.

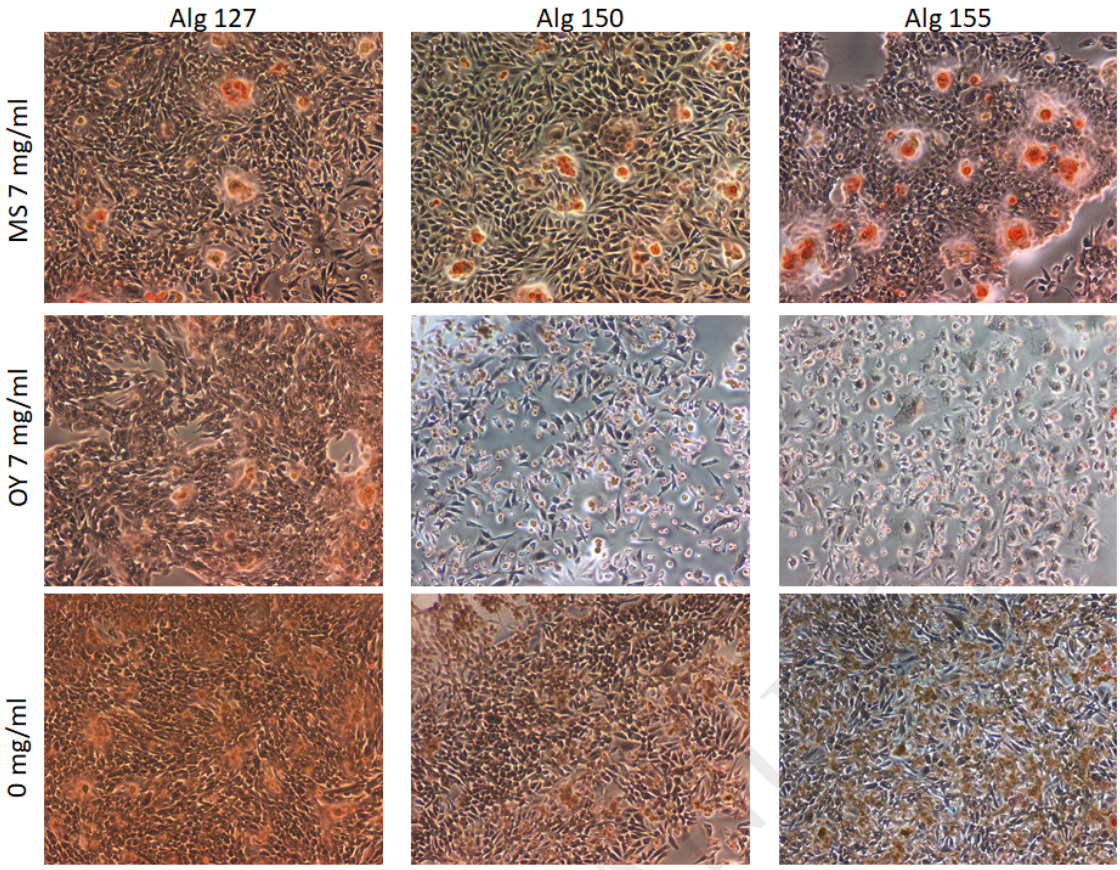

Figure 5: Extracellular matrix mineralization observed by Alizarin Red staining after five days of cell culture with osteoblasts.

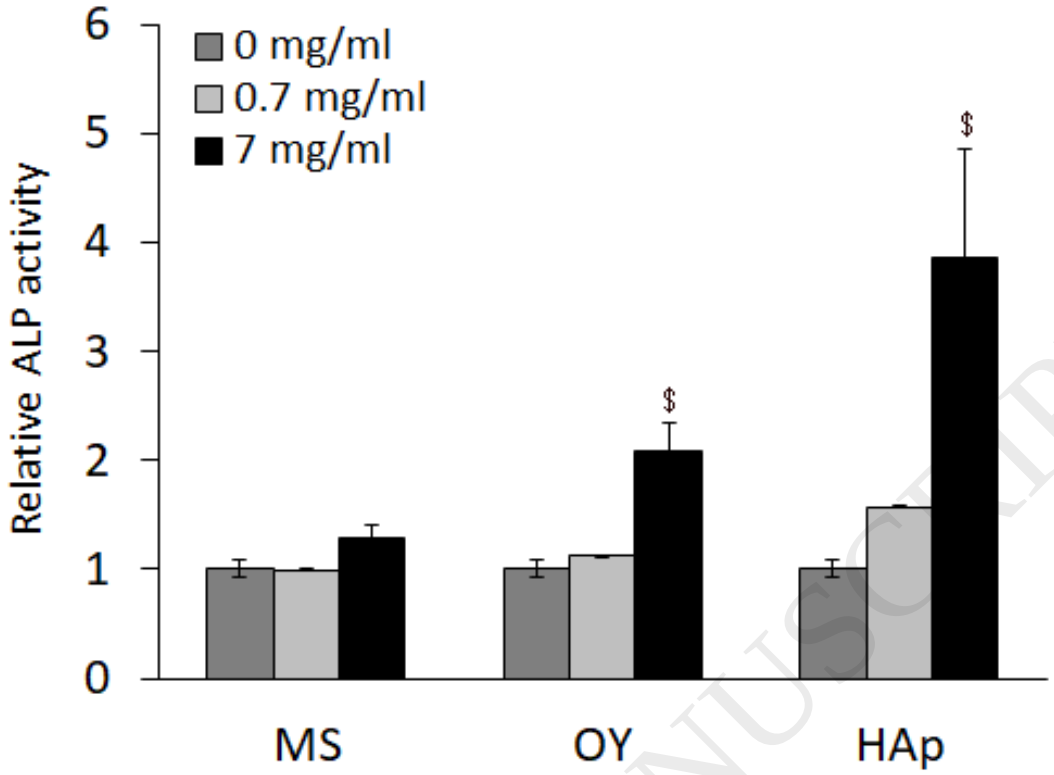

Figure 6: Alkaline Phosphatase activity of human mesenchymal cells cultured on Alginate 155 hydrogels containing variable concentrations of calcium carbonate from mussels (MS) or oysters (OY), or HAp particles. '$' denotes significant difference relative to Alginate 155 alone.

Table 1 H^1-NMR characterization of alginates after partial hydrolysis according to Andriamanantoanina and Rinaudo (Andriamanantoanina & Rinaudo, 2010)

Alginate Type	Recovery of GG (%)	Recovery of MM (%)	M/G Ratio
127	35.35	64.65	0.61
150	40.93	59.07	0.51
155	46.13	53.87	0.55

Table 2 H^1-NMR characterization of alginate blocks obtained after partial hydrolysis of alginates according to Andriamanantoanina and Rinaudo (Andriamanantoanina & Rinaudo, 2010)

Alginate Blocks	Purity(%)	M/G	DPn
127-GG	88	0.06	33.3
150-GG	78	0.04	14.3
155-GG	86	0.04	21.1
127-MM	80	5.67	20.0
150-MM	75	4.26	6.4
155-MM	79	4.56	8.8